A STUDY ON LIQUID SPRAY EVAPORATION INTO A HIGH TEMPERATURE GAS STREAM.

دراسة نبخر قطرات رشة السائل المحقون خلال تيار غازى ذى درجة حرارة عالـــــة.

S. H. El-Emam and M. M. Awad

Department of Mechanical Power Engineering,
Mansoura University, El-Mansoura, Egypt.

خلاصة ــ فى هذا البحث تم تطوير نموذج رياضى لدراسة عملية تبخر قطرات رشة السائل المحقون خلال تيار غازى ذى درجة حرارة عالية ، حيث تم تقسيم المجال الديناميكى للسريان الثنائى الطور إلى خلايا متتابعة وتطبيق معادلات تبادل الحركة والطاقة والمادة بين الغاز وقطرات رشة السائل . وحلت هذه المعادلات باستخدام طريقة الفروق المحدودة والتكامل المتتابع . وقد تم تحديد القيم الأولية لخصائص قطرات رشة السائل والغاز بالاسترشاد بنتائج قياسات معملية . وباستخدام الحاسب الآلى أمكن التوصل إلى دراسة محالات الحركة لكل من الغاز وقطرات رشة السائل وحساب معدل النفير فى التوزيع العددى والحجمى للقطرات وتقدير سرعاتها واتجـــــاه مساراتها وأضا حساب معدل تبخر القطرات . وللتحقق من نتائج الحسابات . تم قيـــــاسى متوسط التوزيع العددى والحجمى لقطرات رشة سائل خلال تيار متدفق من الهواء الساخن علـــى مسافات مختلفة من موضع الرشاش . وتتبر نتائج المقارنة إلى وجود تطابق مناسب من حيـــــث تحدد معدل التغير فى التوزيع العددى والحجمى للقطرات.اعتمادا يدل على أن النموذج المقترح يتمتع بدقة مرضية فى حساب محالات الحركة لكل من الغاز وفطرات رشة السائل وتقدير معــــدل تبخر القطرات .

ABSTRACT -   An analytical model has been developed for the process of liquid spray evaporation into a high temperature gas stream.   In this model, the calculation scheme utilizes the cellular approach in-which each cell is regarded as a control volume and the   gas-droplet interaction is considered. Based on an experimental data, droplets of a liquid spray are classified into several size distribution groups. The conservation laws of mass, momentum and energy are applied to each   group   considering   the   evaporation   and diffusion of droplets. Predictions of gas-droplet flow-field, trajectories of the individual droplets, rate of evaporation and change of size distribution of the spray droplets have been obtained.

An experimental verification of the prediction results has been carrid out. An optical arrangement is used for measurements of sire distribution of spray droplets into a high temperature gas stream. The comparison shows a reasonable agreement of the results based on the analytical model with the experimental measurements for each of droplet size distribution and changes of Sauter mean diameter at different axial distances from the injection nozzle plane.

INTRODUCTION

Evaporation of spray droplets into a high temperature gas stream is an important process in many industrial   applications of   spray systems.   The effectiveness of spray drying systems is dependent on droplet evaporation process.   Fire suppression by sprinkler systems requires fine control of spraying process to produce droplets to be evaporated and penetrated sufficiently enough into the high temperature flame zone. The combustion in the primary zone of a gas turbine combustor is influenced by the atomization, penetration and evaporation processes of the liquid fuel spray. The character of the fuel spray and its evaporation process can also affect the nitric oxide and the carbon monoxide emission levels from spray flames.

Spray parameters, such as mean droplet size, droplet sire distribution and droplet trajectory also gas-flow properties such as pressure, temperature and velocity, are influencing the overall rate of spray evaporation.   Detailed information on the aerodynamics of the gas-droplet flow-field in a given spray system configuration

is essential for prediction of droplet evaporation rate. Such aerodynamic information can be obtained either from measurements or from mathematical simulation of the events taking place in the actual system.

A number of investigators (1) - (4) have presented theoretical analyses for the droplet evaporation problem starting with the droplet heat and mass transfer correlations and the standard drag coefficient curves. Implicit in these analyses is that involving some fairly drastic assumptions which inevitably cast doubt on the validity of the relationshipe obtained. These studies had tended to concentrate on the evapopration of a single droplet, on the ground that it is fundamental to the understanding of the spray as a whole. However, in a spray the evaporation process is far too complex to be regarded merely as an extension of the single droplet case,as reported by Williams (5) and by Rao and Lefebvre (6).

Several studies have been concerned with the evaporation of clouds of spray droplets. Crowe (7) has reported a numerical model for the gas droplet flow-field near an atomizer. Boyson and Swithen-bank (8) have theoretically studied spray evaporation in recir-culating flow. A three dimensional model for gas-droplet of the liquid fuel sprays has been reported by Westbrook (9), but it does not include the effect of droplets on the gas-flow field. Hohsho et al. (10) studied the evaporation process of a group of droplets under substmospheric pressure.

The aim of the present study is to introduce an analytical method for predicting the rate of evaporation of liquid spray droplets into a high temperature gas stream. This incorporates the basic concepts of the mixing-lengh hypothesis of boundary layer and is solved by the finite difference method and the marching integration technique. The basic approach is to determine gas flow-field first, and then proceed to the calculation of trajectories of individual droplets, droplet velocities along these trajectories, rate of droplet evaporation and change of droplet size and droplet size distribution of the spray. Also, an experimental verification of the prediction results is carried out. An optical arrangement developed by El-Emam (11) has been used for measurements of size distribution of spray droplets injected into a high temperature stream of air. A comparison between measured and predicted results of size distribution and changes of the Sauter mean diameter of spray droplets at different axial distances from the injection nozzle plane have been carried out.

Fig. 1 Analytical model.

ANALYTICAL MODEL

The analytical model of liquid spray evaporation into a high temperature gas stream is shown in Fig. 1. The high tem-perature gas stream is introduced co-axially through a duct of cylindrical shape with an axial velocity at the inlet plane. Droplets of the liquid spray are introduced through an injection nozzle symmetrically around the axis of the duct. Based on experimental measurements of spray droplets immediately
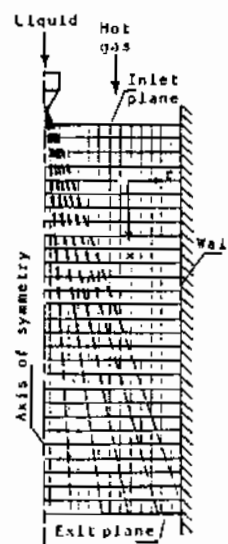
after formation, the spray is divided into five main groups, each group contains (i)th ranges of droplet sizes. The flow-field is sudivided into a series of cells, in-which each cell is considered as a control volume. As droplets traverse a given cell in the flow-field they will exchange momentum and heat with the gas phase contained in the cell and then evaporation is considered from the thermal point of view. The gas-droplet mass, momentum and energy exchanges are treated with an approach based on the BSI-Cell method developed by Crowe et al. (12).

The following assumptions are introduced:

1. The whole flow-field is of the boundary layer type and there is no counter flow occurs.
2. The droplets of the spray are assumed to be spherical in shape.
3. The vapour generated by the evaporation of droplets diffuses into the gas phase in the flow-field.
4. Effect of the gravitational force on the gas phase is negligible.
5. Chemical reaction in the flow-field are not considered.
6. The disintegration region of the spray in the vicinity of the injection nozzle is not considered.

Under these assumptions, the conservation laws of mass, momentum, energy and droplet mass fraction belonging to the (i)th size groups are written on the von Mises plane as the following:

Conservation of mass:

$$\frac{\partial \psi}{\partial x} = - \rho_g v_g r , \qquad \frac{\partial \psi}{\partial r} = \rho_g u_g r \qquad \dots (1)$$

Conservation of axial momentum;

$$\frac{\partial u_g}{\partial x} = \frac{\partial}{\partial \psi} (r^2 \rho_g u_g \mu_{eff} \frac{\partial u_g}{\partial \psi}) - \frac{1}{\rho_g u_g} \frac{\partial p}{\partial x} + \frac{1}{\rho_g u_g} S_U \qquad \dots (2)$$

Conservation of radial momentum;

$$\frac{\partial p}{\partial \psi} = \frac{1}{\rho_g u_g r} S_V \qquad \dots (3)$$

Conservation of energy;

$$\frac{\partial h}{\partial x} = \frac{\partial}{\partial \psi} (\frac{r^2 \rho_g u_g \mu_{eff}}{\sigma_{h,eff}}) + \frac{\partial}{\partial \psi} [r^2 \rho_g u_g \mu_{eff} (1 - \frac{1}{\sigma_{h,eff}}) \frac{\partial (u_g^2/2)}{\partial \psi}] + \frac{1}{\rho_g u_g} S_H \dots (4)$$

Conservation of droplets in the (i)th size group (13);

$$\frac{\partial m_{d,i}}{\partial x} = \frac{\partial}{\partial \psi} (\frac{r^2 \rho_g u_g \mu_{eff}}{\sigma_{d,eff}} \frac{\partial m_{d,i}}{\partial \psi}) + \frac{1}{\rho_g u_g} S_M \qquad \dots (5)$$

where S_U, S_V, S_H and S_M are source terms of axial momentum, radial momentum, energy and vapour mass respectively. m_d is the mass of a droplet.

Based on the Prandtl's mixing-lenght hypothesis, the effective viscosity, μ_{eff} is casted in the following form;

$$\mu_{eff} = \rho_g \, \ell^2 \, (\frac{\partial u_g}{\partial r}) \qquad \ldots \ldots (6)$$

where ℓ, the mixing length, is defined as;

$$\ell = k \, Y_W \qquad \ldots \ldots (7)$$

Y_W is the distance from the wall to the local position and k is a constant=0.435, Ref. (14).

DROPLET EVALUATION

Since the range of the volume fraction of the droplet phase occupation in the cells of the considered flow field is small, the average interdroplet spacing is larger than the gas boundary layer thickness. Therefore the Lagrangian description is adopted to record and analyse the behaviour of each group size of droplets individually. Based on the introduced assumptions mentioned before, a droplet of each size group is subjected to the drag and the gravity forces. The equation of motion for a droplet is given by;

$$m_d \, \frac{d\,\vec{V}_d}{d\,t} = C_D \, \rho_g \, (\,\vec{V}_g - \vec{V}_d\,) \cdot \left| \,\vec{V}_g - \vec{V}_d\,\right| \frac{A_d}{2} + m_d \, \vec{g} \qquad \ldots \ldots (8)$$

where C_D is the drag coefficient, $\vec{V}_g$, $\vec{V}_d$ are gas and droplet velocity vectors, A_d is the droplet area, m_d is the mass of droplet and $\vec{g}$ is the gravity vector.

Based on local measurements in a dilute turbulent two-phase suspension flow, Lee (15) has determined a realistic drag coefficient for droplets over a wide range of flow conditions, that are encountered in this study, where;

$$C_{D,o} = \frac{4}{3} \, \frac{\rho_d}{\rho_g} \, \frac{D \, \vec{g}}{(\,\vec{V}_g - \vec{V}_d\,)^2} \qquad \ldots \ldots (9)$$

For an evaporated droplet, drag coefficient value will be reduced due to mass flux from the surface, for which Bailly et al. (16) suggested the following correlation;

$$C_D = \frac{C_{D,o}}{(\,1 + B\,)} \qquad \ldots \ldots (10)$$

where B is Spalding transfer coefficient given by;

$$B = C_v \, \frac{(\,T_g - T_d\,)}{L} \qquad \ldots \ldots (11)$$

where C_v being the specific heat of the diffusing vapour, T_g and T_d are gas and droplet temperatures, respectively, and L is the latent heat of droplet vaporization.

The rate of change of the temperature of a droplet during its heating up period is estimated ignoring evaporation during this period. If the radiant heat transfer from or to the droplet and the inhomogenous temperature distribution within the droplet are ignored, the following relation is obtained from the heat balance;

$$\frac{dT_d}{dt} = \frac{6\ h}{\rho_g\ C_d\ D}\ (\ T_c - T_d\ ) \qquad \ldots \ldots (12)$$

where C_d is the specific heat of droplet, h is the coefficient of heat transfer which is estimated from the following equation;

$$h = \frac{Nu\ \lambda_g}{D} \qquad \ldots \ldots (13)$$

where λ_g is the heat conductivity of the gas, Nu is the Nusselt number which is taken to vary with the Reynolds number, Re, and the Prandtl number, Pr, and is estimated from the following empirical formula, given by Whitaker as reported by Holman (17);

$$Nu = 2 + (0.4\ Re^{\frac{1}{2}} + 0.06\ Re^{\frac{2}{3}})\ Pr^{0.4}\ (\frac{\mu_g}{\mu_d})^{0.25} \qquad \ldots \ldots (14)$$

Estimation of Reynolds number, Re, of a droplet is based on the relative velocity of the two-phases, where;

$$Re = \frac{\rho_g\ |\vec{V}_g - \vec{V}_d|\ D}{\mu_{eff}} \qquad \ldots \ldots (15)$$

Here, it is assumed that the droplet starts to vaporize when its temperature reaches evaporation temperature (wet-bulb temperature), T_c and that droplet temperature is kept at a constant value through-out the evaporation process.

Based on the heat balance equation between the convection heat and a droplet heat exchanges, the following equation for droplet evaporation temperature, T_e, is reached;

$$T_e = T_g - (\frac{\rho_s\ L}{\rho_g\ C_{p_g}\ (Le)^{\frac{2}{3}}}) \qquad \ldots \ldots (16)$$

where ρ_s is the dry saturated vapour density at T_c and Le is the Lewis number. T_c is estimated using eq. (16) by trial and error.

The rate of vaporization of a spray droplet $\dot{m}_e$ is calculated from the following relation;

$$\dot{m}_e = \frac{\pi\ D\ Nu}{L}\ \lambda_g\ (\ T_g - T_e\ ) \qquad \ldots \ldots (17)$$

Thus the rate of change of decrease of droplet diameter with time ,t, is evaluated from the following equation;

$$\frac{d\ D^2}{d\ t} = -K_e \qquad \ldots \ldots (18)$$

where K_e is the evaporation constant. The values of K_e is estimated from the following equation;

$$K_e = \frac{4 \lambda_d Nu}{L \rho_g} (T_g - T_e) \qquad \ldots \ldots \quad (19)$$

For a droplet traverses a control volume with known location (x,r) and velocity components (u,v) at the upstream cross-section, velocity components at the downstream cross-section can be calculated through Eq. (8), then, the location of the droplet can be calculated by using the next formula;

$$(x , r)_{D.S} = (x, r)_{U.S} + (\frac{u_{U.S} + u_{D.S}}{2} , \frac{v_{U.S} + v_{D.S}}{2}) d t \quad \ldots \ldots \quad (20)$$

where the subscripts D.S and U.S denote downstream and upstream cross-sections of the control volume, respectively.

EXPERIMENTAL APPARATUS

An experimental verification of the prediction results has been carried out. A schematic diagram of the used experimental apparatus is illustrated in Fig. 2. A stream of air is supplied by an air blower [1]. The air flow rate is controlled and measuredthrough a control valve [2] and a metering orifice plate [3], respectively. Then air is preheated up to 130°C by an electric heater [4] installed about 1.5m upstream of the entrance section of the injection duct [5]. The injection duct is made of thin steel with 200 mm in diameter and 500mm in length and is provided with windows to carry out the required measurements. The entrance section of the injection nozzle is designed to ensure an approximately flat velocity distribution of the air. The temperature and the velocity of the air stream are measured with a thermocouple [6] and an impact probe [7], respectively. A liquid water of temperature 25°C is contained in a pressure vessel [10] and injected through an injection nozzle [13] by means of compressed

[1] Air blower
[2] Control valve
[3] Orifice plate
[4] Electric heater
[5] injection duct
[6] Thermocouple
[7] Impact probe
[8] Air compressor
[9] P. control valve
[10] Pressure vessel
[11] Metering burette
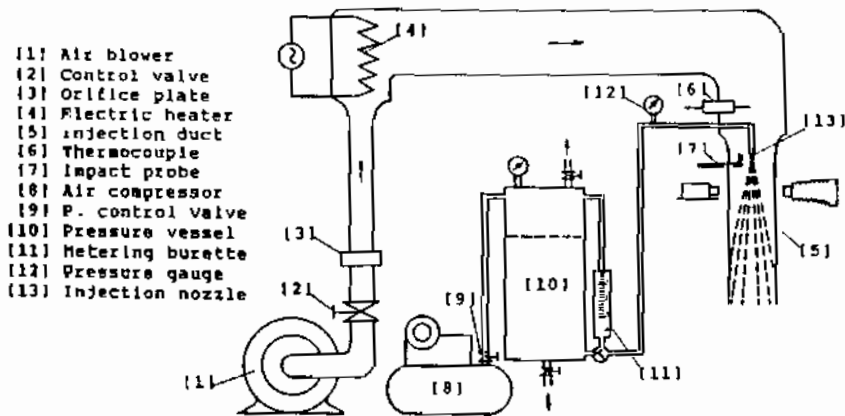[12] Pressure gauge
[13] Injection nozzle

Fig. 2 Experimental apparatus.

air. The injection nozzle is a Delavan swirl pressure type with nominal specifications of; spray cone angle 30° and injection capacity rating 4.5 l/h.   The used compressed air is supplied by the air compressor [8] and controlled through a pressure valve [9] to maintain constant injection pressure during a given experimental period. Injection flow rate and injection pressure rate are monitored through a metering burette [11] and a pressure gauge [12], respectively. Measurements of droplet size distribution immediately after formation as well as at different axial distances from the nozzle plane have been obtained using an optical method developed by El-Emam [11] and described hereafter in Appendix A.

RESULTS AND DISCUSSIONS

Values of initial size distribution and velocity of spray droplets used in the analytical model are taken from the experimental measurements of the droplets immediately after formation at an air stream temperature of 400 K. Since it leads to noticeable error to calculate the mean diameter of droplets directly from the experimental raw data, Sauter mean diameter is estimated after applying Nukiyama-Tanasawa's size distribution function [18]. Typical example of such a calculation process results is shown in Fig. 3 for size distribution of spray droplets immediately after formation. The curve in the figure represents the Nukiyama-Tanasawa's function applied to experimental results histogram.
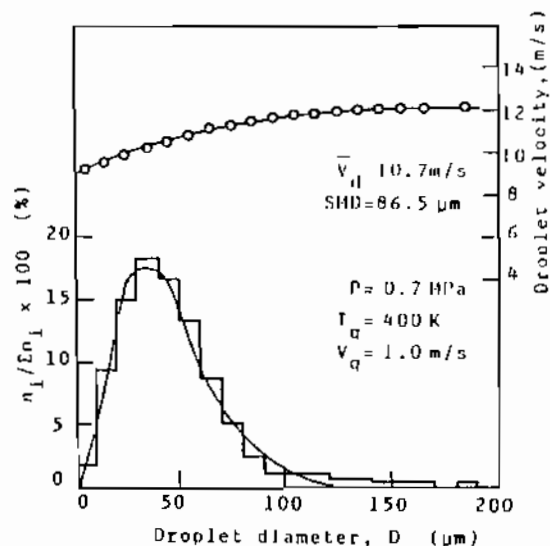

Fig. 3 Size distribution and mean velocity for spray droplets immediately after formation.

In the analytical model shown in Fig. 1, the gas-droplet flow-field inside the injection duct is divided into 40 divisions of equal radial intervals with an integration steps of 0.25 mm in the axial direction.

Based on the experimental results of droplet measurements immediately after formation, shown in Fig. 3, the spray is divided into five main groups, each group contains (1)th size ranges of droplets. Predictions of the spray droplets evaporation process are carried out for different values of the temperature and the velocity of the gas stream.

Comparison between prediction results and experimental measurements of size distribution of the spray droplets at an axial distance x=100mm from the injection nozzle plane is shown in Fig. 4. The predicted results show a reasonable agreement with the experimental measurements in the trend of the size distribution curves and the locations of their peaks. Fig. 5 shows a comparison between prediction and experimental results of the changes of Sauter mean diameter against the axial distance from the injection nozzle plane. The figure shows that there is an agreement in the tendency of the predicted and the measured results of the rate of change of the Sauter mean diameter due to droplet evaporation process.
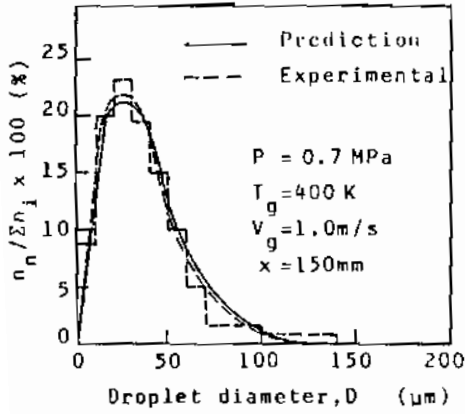
Fig. 4 Predicted and measured
        size distributions of
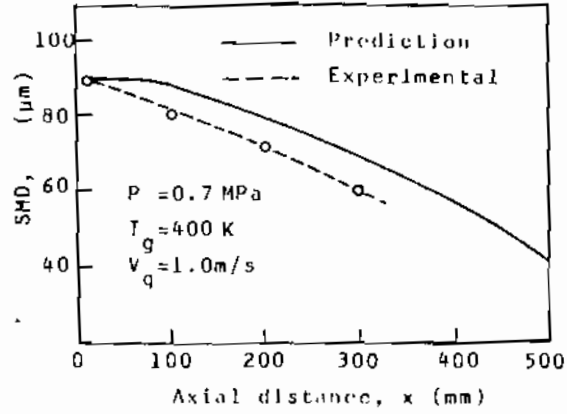   a spray droplets.

Fig. 5 Predicted and measured
        changes of the Sauter
        mean diameters.

Predicted results of the radial profiles of the gas stream
velocity at different axial distances are shown in Fig. 6.   It can
be noted that gas velocities inside the spray are higher than those
outside the spray and have a maximum values near the axis of the
spray.   Also, gas velocity inside the spray decreases with increase in
the axial distance from the injection nozzle plane.

Influence of gas temperature on predicted average values of
the evaporation rate of spray droplets, as represented by $\bar{K}_e$, in mm^2/s,
for variant gas velocities at different axial distances is shown in
Fig. 7. Generally, it can be noted that increase in gas temperature
raises spray evaporation rate. Evaporation rate increased almost
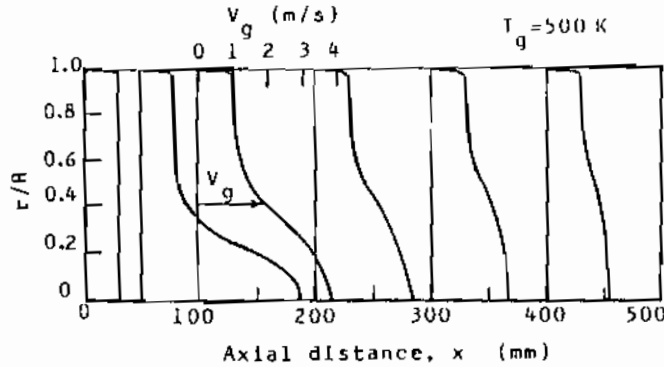

Fig. 6 Predicted profiles of gas stream velocity
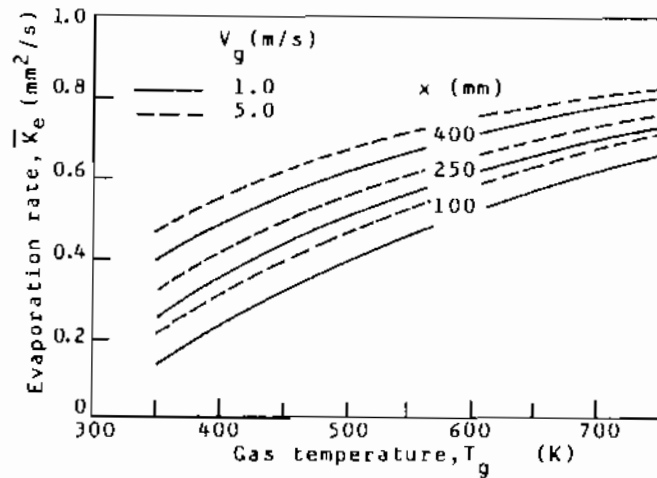   at different axial distances.

Fig. 7 Influence of gas temperature on predicted
        spray evaporation rate.

lineary with gas temperature until about 550K. At higher temperatures,
the effect of increase in gas temperature on spray evaporation is
decreased. Also, the figure shows that evaporation rate of the spray
is increased with increase in the axial distance and the velocity of
the gas stream. When a spray is injected into the gas stream, the
droplets may accelerate or decelerate to the stream velocity, depend-
ing upon the relative velocity and the drag coefficient. Evaporation
rates of droplet are higher during this initial stage, when the rela-
tive velocity is high, than at later stages when the relative velocity
becomes negligible. However, as the axial distance increases, the mean
droplet size reduces and therby increase the droplet surface area and
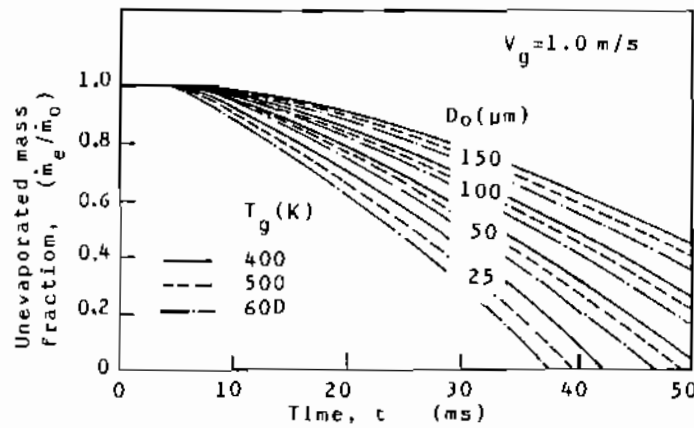hence spray evaporation rate.

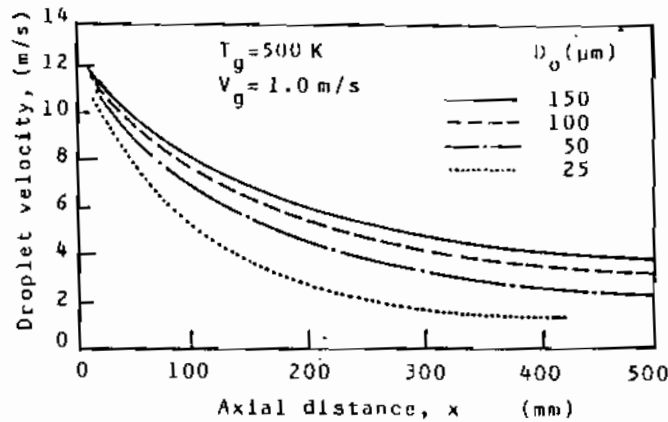Fig. 8 Predicted unevaporated mass fraction against time.

Fig. 9 Predicted mean velocities of spray droplets.

Profiles of predicted results of unevaporated mass fraction against time at different values of the gas stream temperature for droplets of different size groups are shown in Fig. 8. As expected, the evaporation rate of droplets with decrease in droplet size group. Also, the heating-up time of a droplet becomes shorter and the evaporation rate increases with increase in gas stram temperature as well as decrease in droplet size. These results are in good agreement with the experimental results observed by Chigier et al. (19).

Predicted results of the change of mean velocities for droplets of different size groups against the axial distence are shown in Fig. 9 From the figure, it can noted that small droplets lose their momentums and reach their terminal velocities early while large size droplets move with higher velocities inside the spray.

Predicted results of flight trajectories of individual size group droplets are shown in Fig. 10. Droplets of the spray are spread-out with different flight trajectories depending on the influence of the drag force on each size group. Droplets of small sizes are inclined towards the inside of the spray. Also, the figure shows that small size droplets are evaporated completely early while large droplets move away and hit the wall of the injection duct.
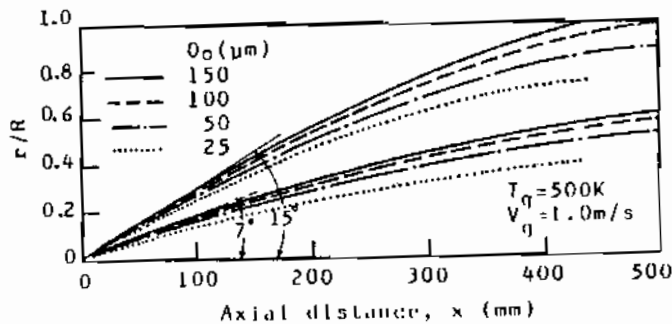

Fig. 10 Predicted trajectories of spray droplets.

CONCLUSIONS

        An analytical model has been developed to describe the process
of liquid   spray evaporation into a high temperature gas stream.
Predictions of gas-droplet flow-field, trajectories of the individual
dropletd, droplet evaporation rate and changes of droplet sizes have
been obtained. An experimental verification of the prediction results
has been carried out.   Although the prediction results can only be
considered as semiquantitative, a number of general conclusions can be
drawn;

1. The comparison shows a reasonable agreement of the results based
   on the analytical model with the experimental measurements for each
   of droplet size distribution and changes in Sauter mean diameter at
   different axial distances from the injection nozzle plane.
2. Velocities of the gas stream inside the spray are higher than
   outside the spray ..and it has maximum values near the axis of the
   spray.
3. Droplets of the spray are spread-out with different flight trajec-
   tories depending upon the influence of the drag force on each size
   group.
4. Droplets of small size loose their momentum and reach their terminal
   velocities early while droplets of large size move away with higher
   velocity.
5. The heating-up time of a droplet becomes shorter with increase in
   gas stream temperature and with decrease in droplet size.
6. Evaporation rates of spray droplets increase with increase in gas
   stream temperature, gas stream velocity and axial distance and with
   decrease in droplet sizes.

NOMENCLATURE

A   : Area
B   : Spalding transfer coefficient
C   : Specific heat
C_D : Drag coefficient
D   : Droplet diameter
$\vec{g}$: Gravity vector
h   : Specific enthalpy or coefficient of heat transfer
K_e : Evaporation constant
L   : Latent heat of vaporization
ℓ : Mixing length
m   : Mass
N   : Number of droplets
Nu   : Nusselt number
P   : Pressure
Pr   : Prandtl number
r   : Radial coordinate
Re   : Reynold's number
S_H : Source term of energy
S_M : Source term of vapour mass
S_U : Source term of axial momentum
S_V : Source term of radial momentum
SMD : Sauter mean diameter
T   : Temperature
t   : Time
u   : Velocity component in x direction
$\vec{v}$: Velocity vector
v   : Velocity component in r direction
x   : Axial coordinate

Greek Symbols

λ : Heat conductivity
ρ : Density
ψ : Stream function
μ_{eff} : Effective viscosity
$\sigma_{h,eff}$: Effective Prandtl number
$\sigma_{d,eff}$: Effective Schmidt number

Subscripts

d : Droplet
e : Evaporation
g : Gas
D.S : Down-stream
o : Reference value
s : Surface
U.S : Up-stream
v : Vapour

REFERENCES

1. Hoffman, T.W. and Gauvin, W. H., An Analysis of Spray Evaporation in a High Temperature Environment, The Canad. Journal of Chemical Eng., Vol. 40, (1962), 110.
2. Hedley, A. B., Muruzzman, A.S. and Martin, G. F., Combustion of Single Droplets and Simplified Spray Systems, Journal of the Inst of Fuel, Vol. 44, (1971), 38.
3. Ohta, Y., Shimoyama, K. and Ohigashi,S., Vaporization and Combustion of Single Liquid Fuel Droplets in a Turbulent Environment, Bull. of the JSME, Vol. 18, No. 115, (1975), 47.
4. Kodata, T. and Hiroyasu,H., Evaporation of a Single Droplet at Elevated Pressures and Temperatures, Bull. of the JSME, Vol. 19, No. 138, (1976), 1515.
5. Williams, A., Combustion of Droplets of Liquid Fuel, a Review, Combustion and Flame, Vol. 21, (1973), 1.
6. Rao, K. V. L. and Lefebvre, A.H., Evaporation Characteristics of Kerosine Sprays Injected Into a Flowing Air Stream, Combustion and Flame, Vol. 26, (1976), 303.
7. Crowe, C.T., A Numerical Model for Gas-Droplet Flow-Field Near an Atomizer, Proc. of 1st ICLASS, Tokyo, (1978), 377.
8. Boyson, F. and Swithenbank,J., Spray Evaporation in Recirculating Flow, Proc. of 17th Int. Symp. on Combustion, Leeds, (1979), 443.
9. Westbrook, C. K., Three-Dimensional Numerical Modeling of Liquid Fuel Sprays, Proc. of 16th Int. Symp. on Combustion, the Combustion Inst., (1977), 1517.
10. Nohsho, Y., Kodata, T., Kadowaki, K., Makino, K. and Kotera, S., Evaporation of a Group of Droplets under Subatmospheric Pressure, Bull. of JSME, Vol. 29, No. 255, (1986), 3D21.
11. El-Emam, S. H., A Photographing Method for Measurements of Spray Droplets Immediately after Formation, Bull. of the Faculty of Eng., Mansoura Univ., Vol. 11, No. 1 , (1986), M62.
12. Crowe, C.T., Sharma, M.P. and Stock, D.E., The Particle-Source-in Cell(PSI-Cell) Model for Gas-Droplets Flows, Trans. ASME (J. of Fluids Engineering), Vol. 99, (1977), 631.
13. Katsuki, M., Mizutani, Y., and Ohta, M., Theoretical Approach to Spray Combustion in Gas Turbine Combustor, Technology Report of the Osaka Univ., Vol. 29, No.1482, (1979), 205.

14. Patankar, S. V. and Spalding, D.B., Heat and Mass Transfer in
     Boundary Layers, 2nd Ed., Intertext Book, (1970), 74.
15. Lee, B. L., Particle Drag in a Dilute Turbulent Two-Phase Suspen-
     sion Flow, Int. J. Multiphase Flow, Vol. 13, No. 2, (1987), 247.
16. Bally, G. H., Slater, I.W. and Eisenklam, P., Dynamic Equations
     and Solutions for Particles Undergoing Mass Transfer, Brit. Chem.
     Eng., Vol. 15, No. 7, (1970), 912.
17. Holman, J.P., Heat Transfer, 6th Ed., McGraw Hill, (1986), 220.
18. Nukiyama, S. and Tanasawa, Y., An Experimental on the Atomization
     of Liquid (3rd Report on the Distribution of the size of Droplets)
     Trans. JSME, Vol. 5, No. 18, (1939), 131.
19. Chigier, N.A. and McCreath,C.G., Combution of Droplets in Sprays,
     Acta Astronautica, Vol. 1, (1974), 687.

Appendix A

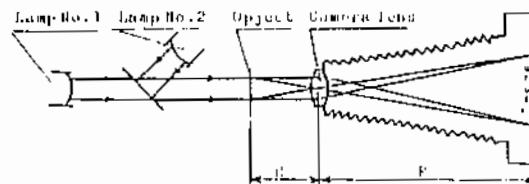### The Optical System for Droplet Measurements

Fig. 11 Optical system

The arrangement of the optical system used for droplet measurements is shown in Fig. 11. In this system, a 50 mm Nikkor lens, f 1/2 mounted in-reverse on an adapter attachment, was fitted to a Nikon FE camera with an extension bellows. A graticule scale mounted to a traverser was placed in the plane of focus to calibrate and determine characteristics of the optical system. Results of the measured characteristics of the optical system are shown in Fig. 12. Two micro-stroboscopes were used to give two flashes of light, one firing after the other. The light beams were aligned in the same direction by using a half-silvered mirror as a beam splitter. The interval between the two flashes was controlled by an electronic time delay unit. The interval between flashes was choosen so that complete separation of the images was achieved for most of the image pairs.

An example of droplets image photographs is shown in Fig. 13. Data obtained from such photographs were corrected for its count to any bias and then processed through a computer program to calculate droplet size distribution, Sauter mean diameter, mean velocity and mean flight direction.
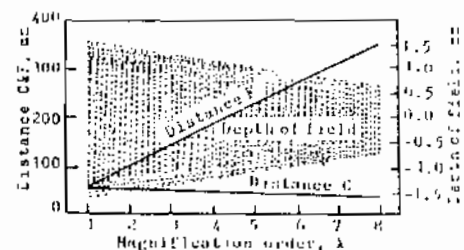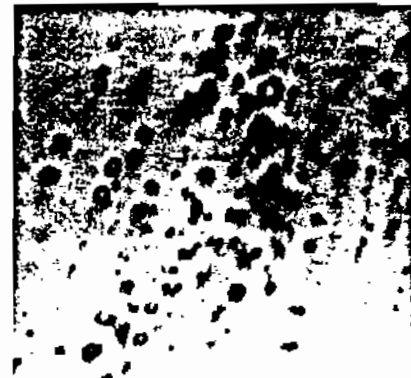

Fig. 12 Characteristics of the optical system.

Fig. 13 Example of droplet photographs.